Supplementary Figure 1

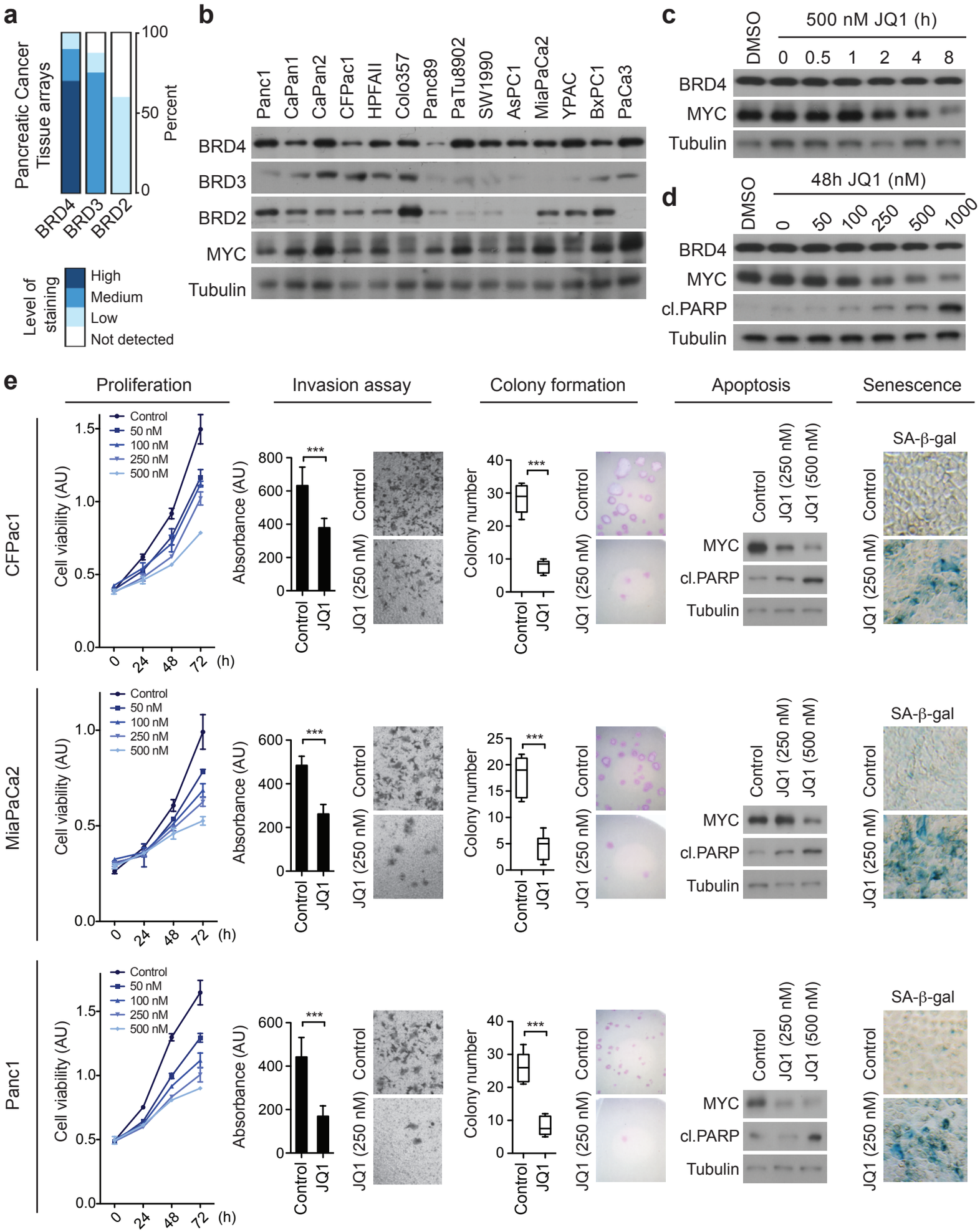

Supplementary Figure 1. The BET bromodomain inhibitor JQ1 blocks cell growth, inhibits invasion and colony formation, and induces apoptosis and senescence in pancreatic cancer cells *in vitro*.

(**a**) BET proteins expression in human pancreatic cancer tissue array (proteinatlas.org).

(**b**) BET bromodomain proteins are expressed in human PDAC cell lines. MYC levels are shown and Tubulin serves as a loading control in this immunoblot.

(**c**) JQ1 treatment (8h) inhibits MYC expression by immunoblot analysis in CFPac1 cells.

(**d**) JQ1 treatment leads to reduced MYC expression and induced apoptosis (measured by cleaved PARP) in a dose-dependent manner in CFPanc1 cells by immunoblot analysis.

(**e**) Cellular assays on a panel of human PDAC cell lines in response to JQ1 treatment. Proliferation was measured by the MTT assay. MYC levels and cleaved PARP levels (apoptosis) are shown by immunoblot. Senescent cells are marked by SA-β-galactosidase after 48h of drug treatment. Each assay represents at least 3 independent replicates.

***: $P < 0.001$; n.s.: not significant (two-tailed unpaired Student's t-test). Data are represented as mean +/– SEM.

Supplementary Figure 2

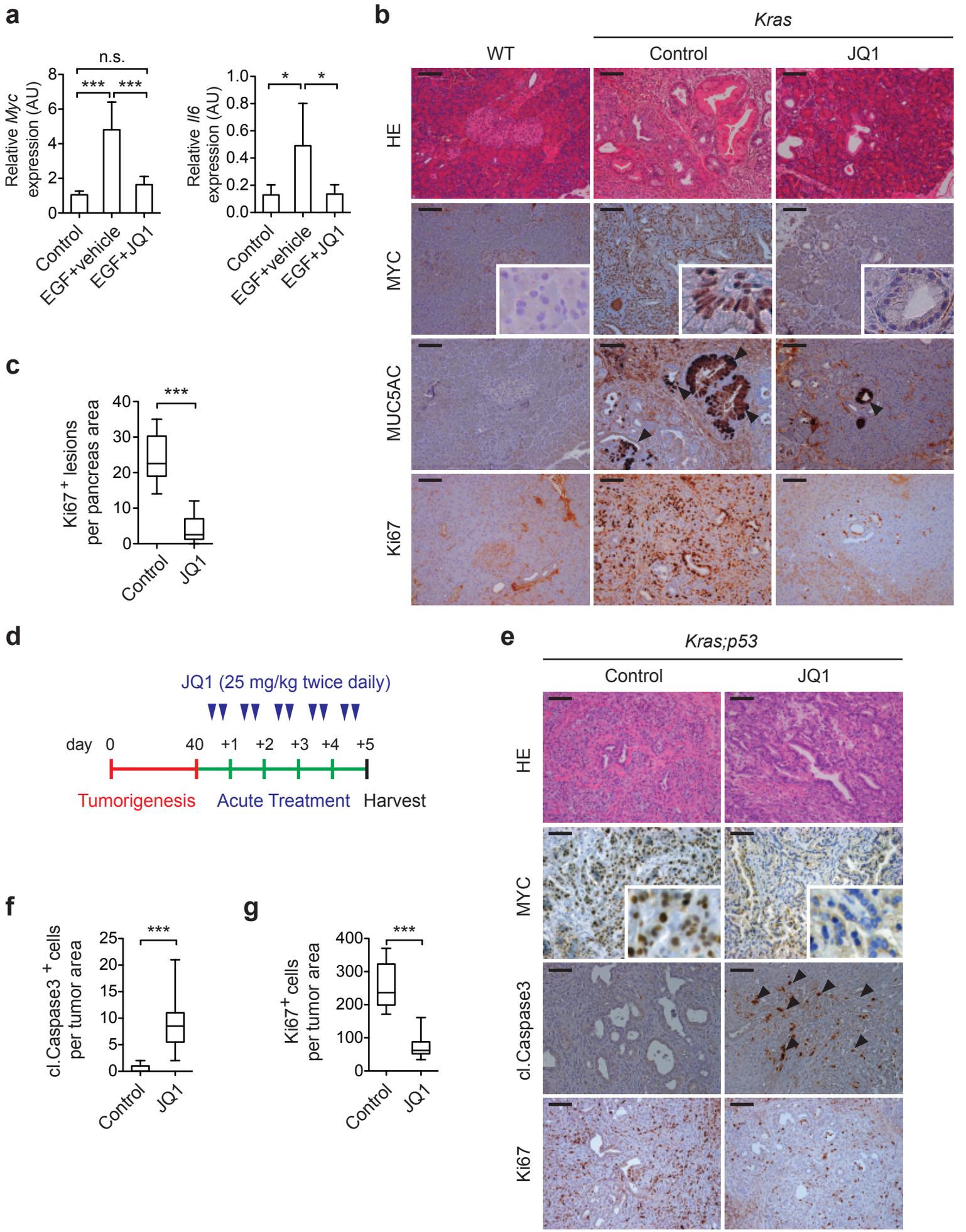

Supplementary Figure 2. JQ1 blocks pancreatic tumor initiation and acute treatment inhibits advanced PDAC *in vivo.*

(**a**) Quantitative real-time-PCR (qRT-PCR) analysis of *Myc* expression at day 3 of control- and EGF-induced and JQ1-treated ADM *ex vivo* explant cultures (four independent biological replicates). ***: $P < 0.001$; n.s.: not significant (two-tailed unpaired Student's t-test). Data are represented as mean +/– SEM.

(**b**) Representative HE staining and IHC for MYC, MUC5AC, a marker of PanIN lesions (arrowheads), and Ki67, a marker of proliferation in *Kras* mutant mice in response to JQ1 treatment; wild-type (WT) sections are shown as a control. Scale bars, 50 μm.

(**c**) Quantification of proliferation (Ki67 positive cells) in caerulein-treated pancreata from *Kras* mutant mice treated with JQ1 (n = 6 for each experimental group). ***: $P < 0.001$ (two-tailed unpaired Student's t-test). Data are represented as mean +/– SEM.

(**d**) Schematic of acute JQ1 treatment protocol in *Kras;p53* mutant mice.

(**e**) Representative HE staining and IHC for MYC, cleaved Caspase 3 (cl.Caspase3) a marker of apoptosis (arrowheads), and Ki67, a marker of proliferation in control and acute JQ1 treated PDAC. Scale bars, 50 μm.

(**f–g**) Quantification of apoptotic cells (f) (Cl.Caspase3) and proliferation (g) in acute JQ1 treatment of advanced PDAC tumors in *Kras;p53* mutant mice (n = 5 for each experimental group). ***: $P < 0.001$ (two-tailed unpaired Student's t-test). Data are represented as mean +/– SEM.

Supplementary Figure 3

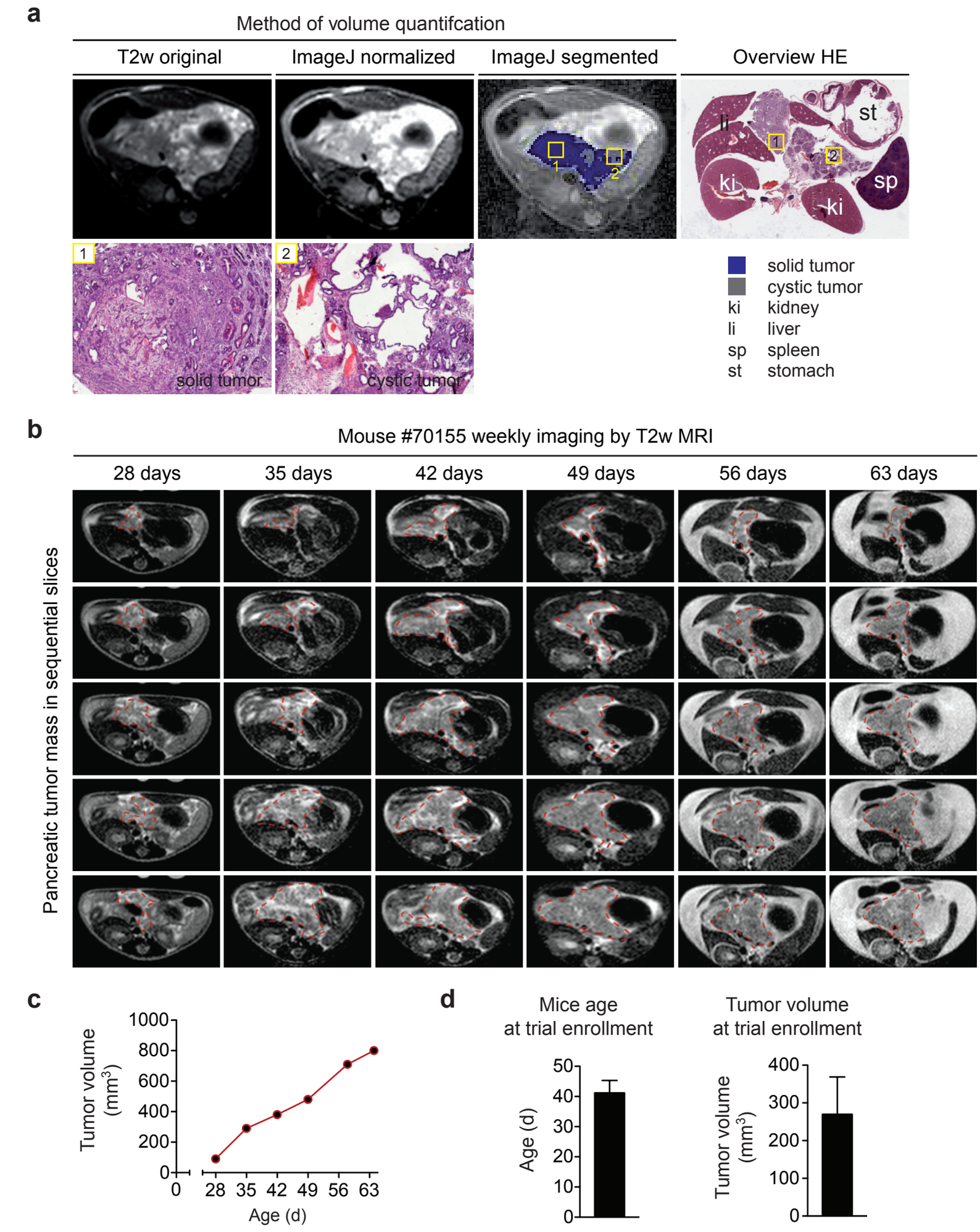

Nature Medicine: doi:10.1038/nm.3952

Supplementary Figure 3. Tumor development and progression monitored by T2-weighted MRI correlates with tumor histopathology.

(**a**) Correlation of T2w MRI and ImageJ-based segmentation for accurate volume quantification is shown with tumor histomorphology. A tissue processing procedure was developed to preserve organ localization as found *in situ* for optimal comparison with the MRI data sets.

(**b**) Weekly imaging by T2w MR imaging shows PDAC growth in a *Kras;p53* mutant mouse. Note development of ascites at day 56 and 63 (white appearance)

(**c**) Quantification of tumor growth. Mice were included into trials with a volume of approximately 200–400 mm^3 (med.=251mm^3).

(**d**) Average age and tumor volume of *Kras;p53* mutant mice enrolled in the treatment trials (n = 39).

Supplementary Figure 4

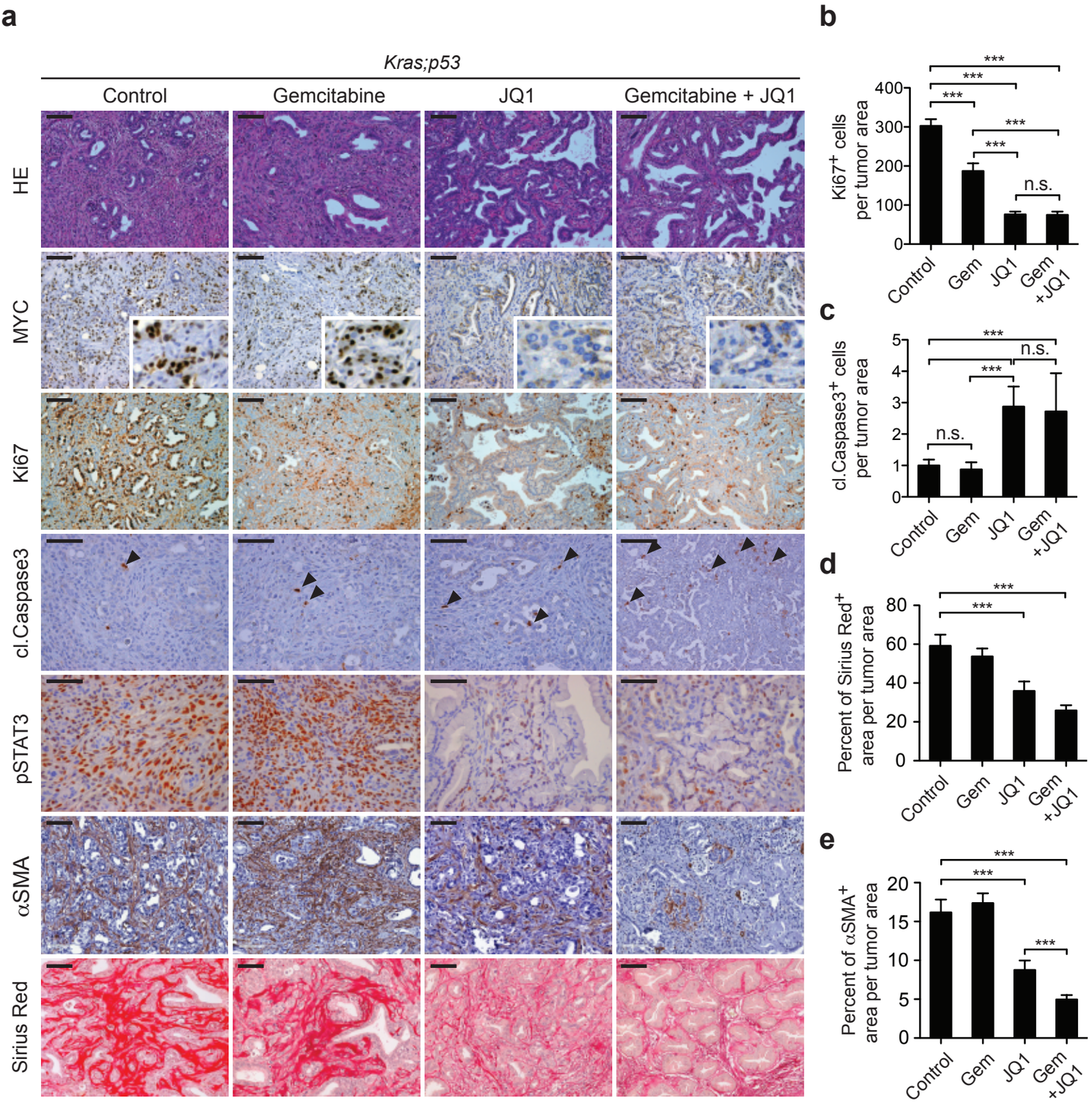

Nature Medicine: doi:10.1038/nm.3952

Supplementary Figure 4. BET bromodomain inhibition with JQ1 blocks PDAC *in vivo*.
(**a**) Representative HE staining and IHC for MYC, Ki67 (a marker of proliferation), cleaved Caspase 3 (cl.Caspase3, a marker of apoptosis - arrowheads), pSTAT3, αSMA (a marker of myofibroblasts/stellate cells) and Sirius Red (a marker of stromal fibrotic deposit) in control and treatment groups. Scale bars, 50 μm.
(**b–e**) Quantification of proliferation (b) (Ki67), apoptosis (c) (cl.Caspase3) and tumor-associated stroma (d - αSMA, and e - Sirius Red) (n = 5 for each experimental group). ***: $P < 0.001$; n.s.: not significant (two-tailed unpaired Student's t-test). Data are represented as mean +/– SEM.

Supplementary Figure 5

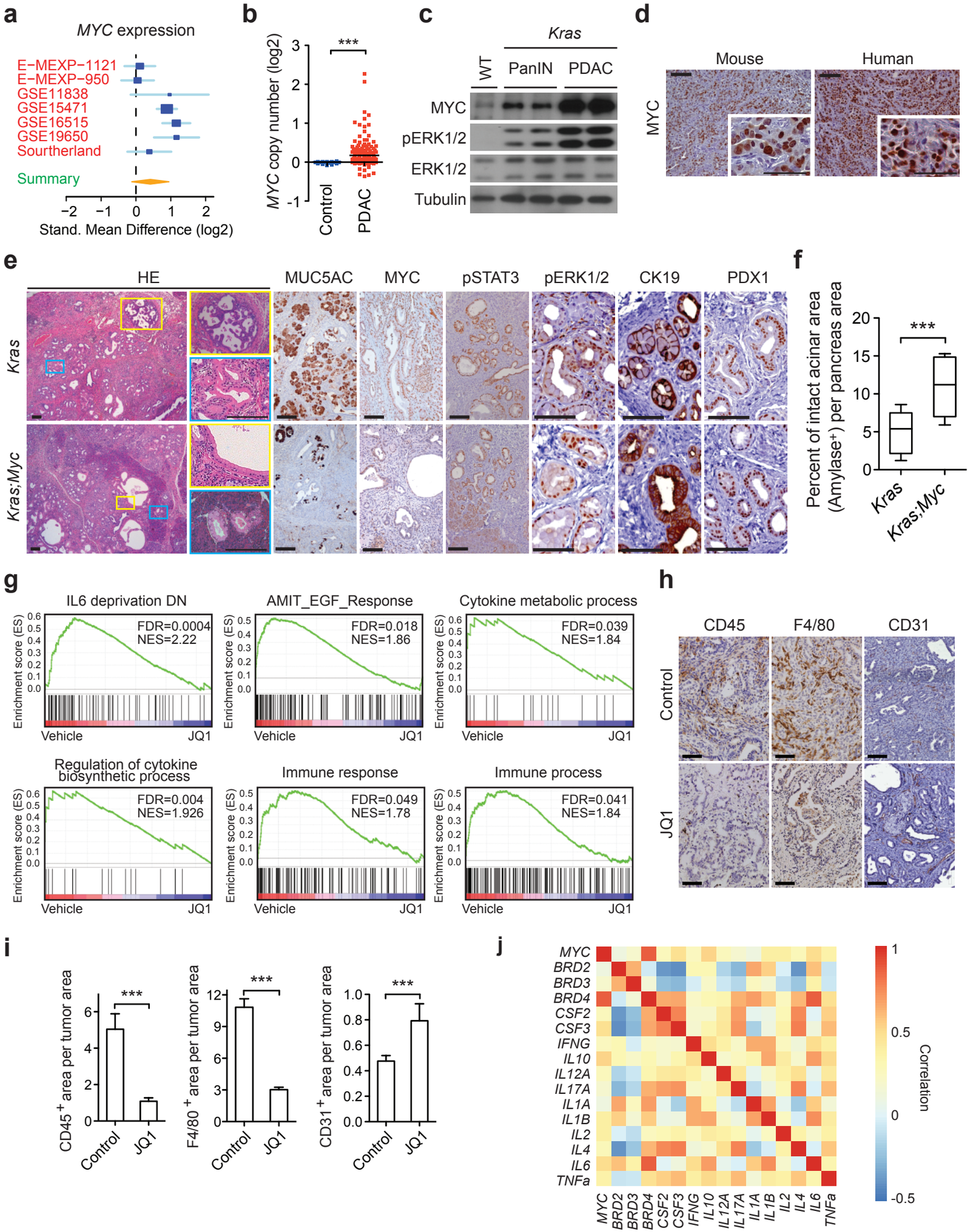

Supplementary Figure 5. *MYC* is commonly amplified and overexpressed in human PDAC, *Myc* deletion attenuates pancreatic tumorigenesis *in vivo* and JQ1 treatment inhibits inflammation in PDAC.

(**a**) Summary of *MYC* expression levels in seven publically available human PDAC expression datasets (n = 203 PDAC samples and n = 91 normal pancreas samples). Detailed statistical description in the Methods section.

(**b**) Analysis of TCGA data for *MYC* copy numbers in PDAC. ***: $P < 0.001$ (two-tailed unpaired Student's t-test).

(**c**) Immunoblot analysis with the indicated antibodies on tumor lysates from wild-type pancreas and from the pancreas of *Kras* mutant mice at 4.5 and 9 months of age when mice develop PanIN and PDAC, respectively (each time point represents two biological replicates).

(**d**) Immunohistochemical analysis of MYC expression in mouse and human PDAC. Scale bars, 50 μm.

(**e**) Analysis of pancreatic tumorigenesis at 6 months in *Kras* and *Kras;Myc* mutant mice. Representative histology section (HE), IHC for the PanIN marker MUC5AC, MYC, pSTAT3, pERK1/2 and tumor markers CK19 and PDX1. Pancreatic cancer phenotypes in *Kras* mice show preneoplastic (PanIN) lesion development in the whole organ (blue insert) and local advanced PanIN3-carcinoma *in situ* (yellow insert). *Kras;Myc* mutant mice show low grade PanIN development with areas of intact pancreas. Scale bars, 50 μm.

(**f**) Quantification of intact normal acinar area (Amylase positive area) in *Kras* and *Kras;Myc* mutant mice. Data are represented as mean +/– SEM. ***: $P < 0.001$ (two-tailed unpaired Student's t-test).

(**g**) GSEA on datasets obtained from primary PDAC cells treated with JQ1 and vehicle controls.

(**h**) IHC staining of CD45 (leukocyte common antigen), F4/80 (macrophages), and CD31 (endothelial cells) in control and JQ1-treated tumors. Scale bars, 50 μm.

(**i**) Quantification of b (n = 5 for each experimental group). ***: $P < 0.001$ (two-tailed unpaired Student's t-test). Data are represented as mean +/– SEM.

(**j**) Heatmap representation of Pearson correlations between expression of bromodomain coding genes (*BRD2, BRD3, BRD4, BRDT*), *MYC*, and various cytokines in a human pancreatic cancer expression gene set (GSE15471).

Supplementary Figure 6

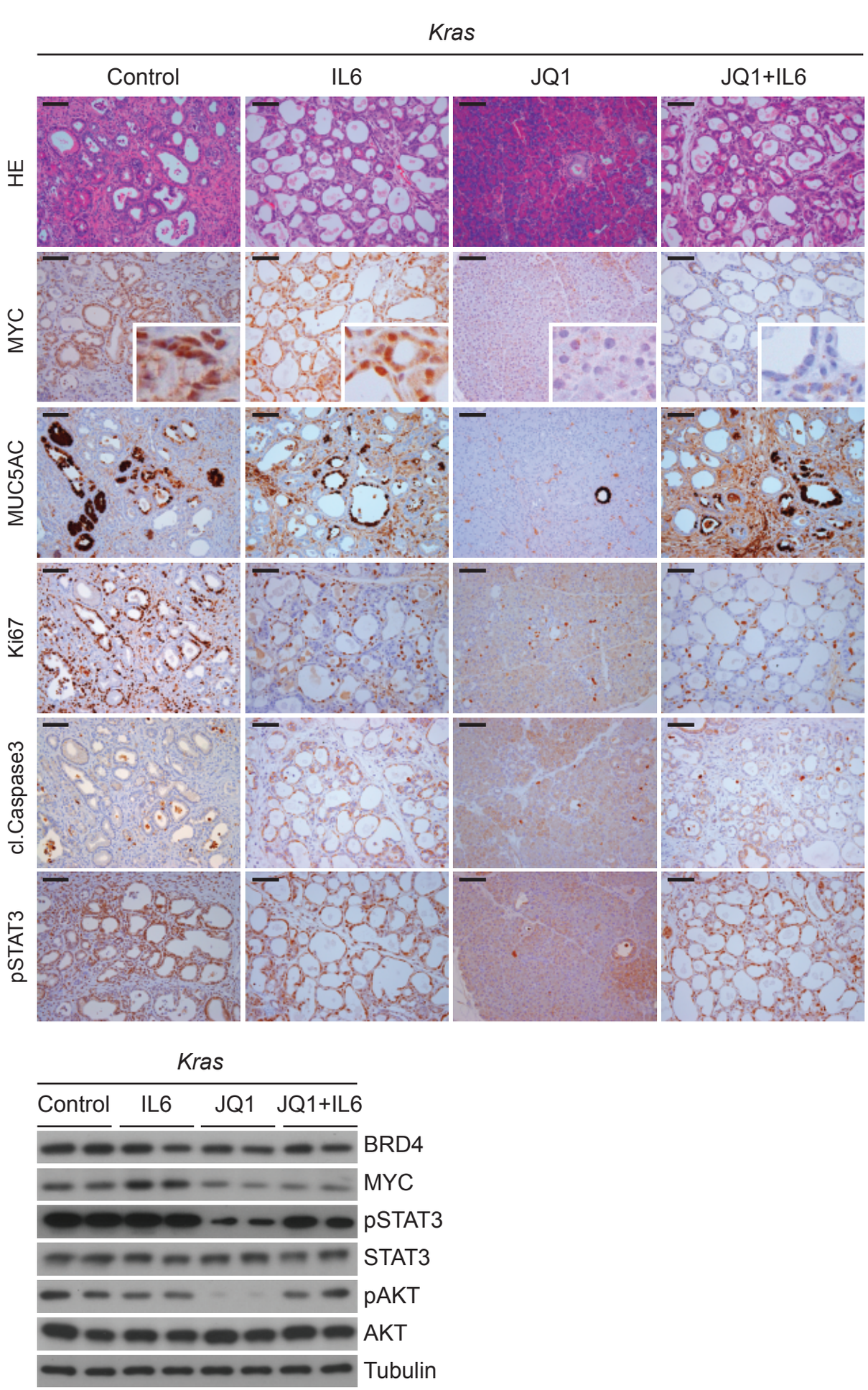

Supplementary Figure 6. Treatment with exogenous IL6 prevents the tumor-inhibitory effects of JQ1 treatment on PDAC *in vivo*.
(**a**) Representative HE staining and IHC for MYC, Ki67 (a marker of proliferation), cleaved Caspase 3 (cl.Caspase3, a marker of apoptosis - arrowheads), MUC5AC (a marker of PanINs), and pSTAT3 in control and treatment groups. Scale bars, 50 μm.
(**b**) Immunoblots analysis of tumor lysates in *Kras* mutant mice (each treatment group represents two biological replicates).

Nature Medicine: doi:10.1038/nm.3952

Supplementary Figure 7

a

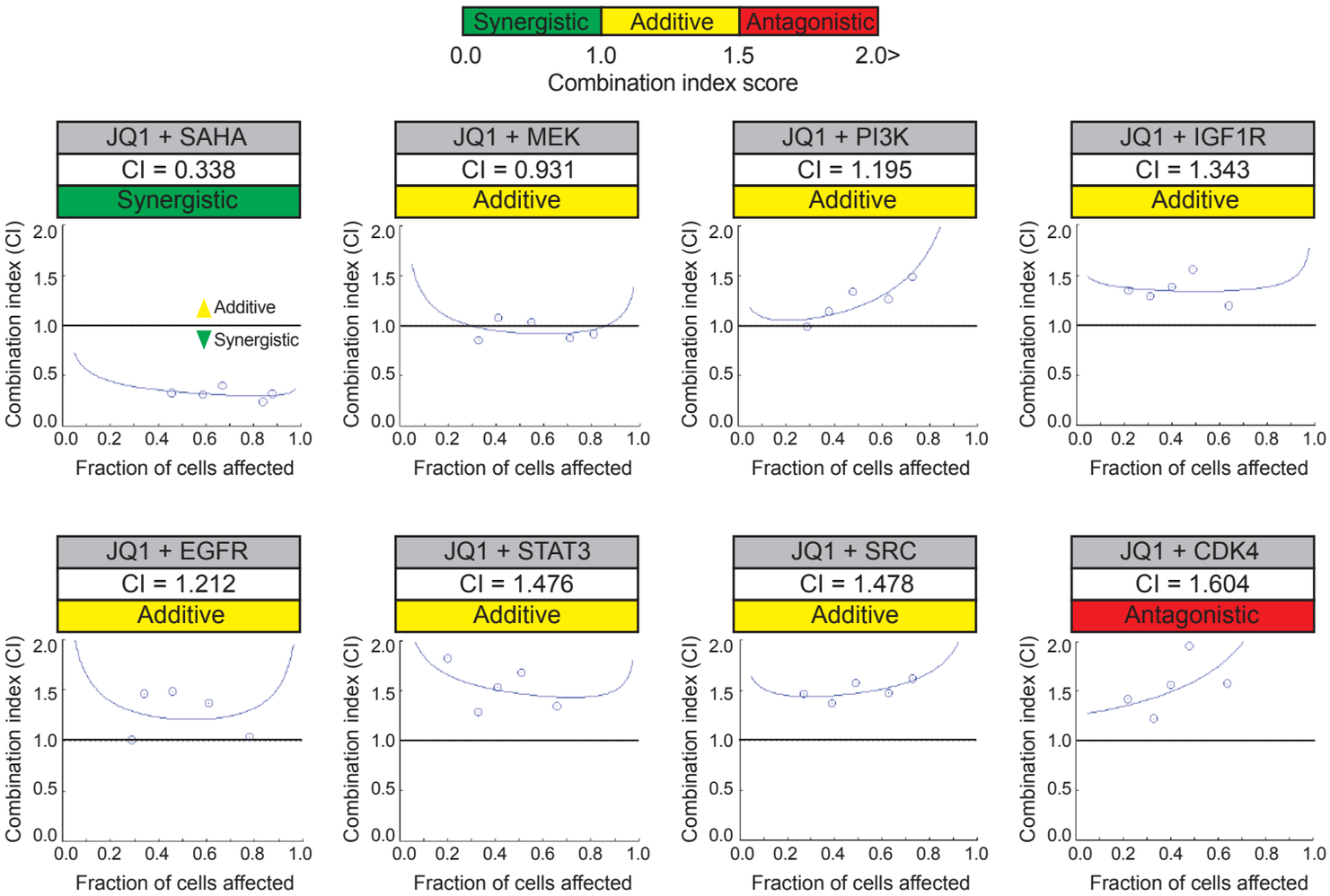

b

	JQ1		SAHA		JQ1+SAHA
Cell line	IC50 (nM)	95% CI	IC50 (nM)	95% CI	Combination index (CI)
W22-PPT	606.7	233.6 to 1576	2703	1.341 to 5.450	< 0.09
5436-PPT	291.9	128.4 to 663.5	8498	1.516 to 47.62	< 0.05
DanG	474.1	210.7 to 1066.5	2824	0.4887 to 16.32	< 0.13
Panc1	222.3	155.2 to 318.3	1115	0.01618 to 3.107	< 0.92

Supplementary Figure 7. A drug combination screen identifies synergistic effects in PDAC cells.

(**a**) Combination index (CI) scores of a drug synergy screen performed in CFPac1 cells using 8 inhibitors and JQ1: BETi (JQ1), HDACi (SAHA), MEKi (CI1040), PI3Ki (GDC0941), IGF1Ri (OSI-906), EGFRi (Erlotinib), STAT3i (Stattic), SRCi (AZD0530) and CDK4i (PD0332991). CI scores were derived as described in the Methods and categorized as synergistic (CI<1), antagonistic (CI>1.5) or additive (1<CI>1.5). Each CI score represents data from 5 different drug doses of single and paired-drug treatments with 4 biological replicates per condition.

(**b**) Combination index (CI) scores in the indicated PDAC cell lines.

Supplementary Figure 8

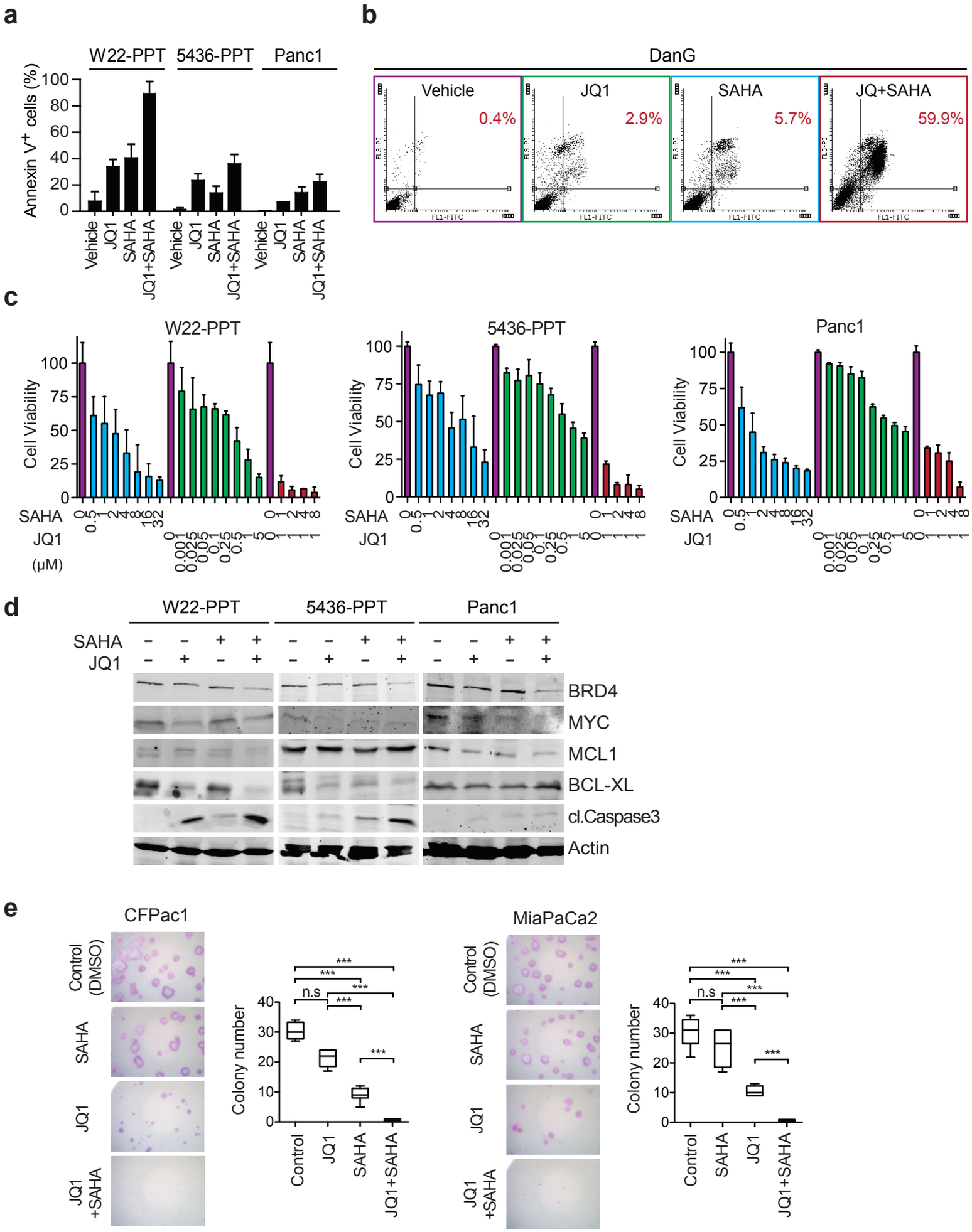

Supplementary Figure 8. Synergistic inhibitory effects of JQ1 and SAHA treatment on PDAC cells *in vitro.*

(**a**) The indicated PDAC cell lines were treated with 250nM of JQ1 and/or 250nM of SAHA for 72h. Apoptosis was quantified by Annexin V staining.

(**b**) FACS analysis of Annexin V staining (as in a and in Fig. 3c).

(**c**) PDAC cell lines represent two independent biological replicates treated in triplicate with the indicated concentrations of JQ1 and SAHA for 72h and viability was measured by the MTT assay and is shown relative to untreated controls for each cell line. Error bars represent SEM for each measurement.

(**d**) PDAC cell lines were treated with SAHA and/or JQ1 for 24h. Lysates were probed with the indicated antibodies for immunoblot analysis.

(**e**) Representative pictures of colony formation assays in response to JQ1 (250nM) and/or SAHA (250nM) treatment. Quantification is shown for three replicates for each treatment group. ***: $P < 0.001$; n.s.: not significant (two-tailed unpaired Student's t-test). Data are represented as mean +/– SEM.

Supplementary Figure 9

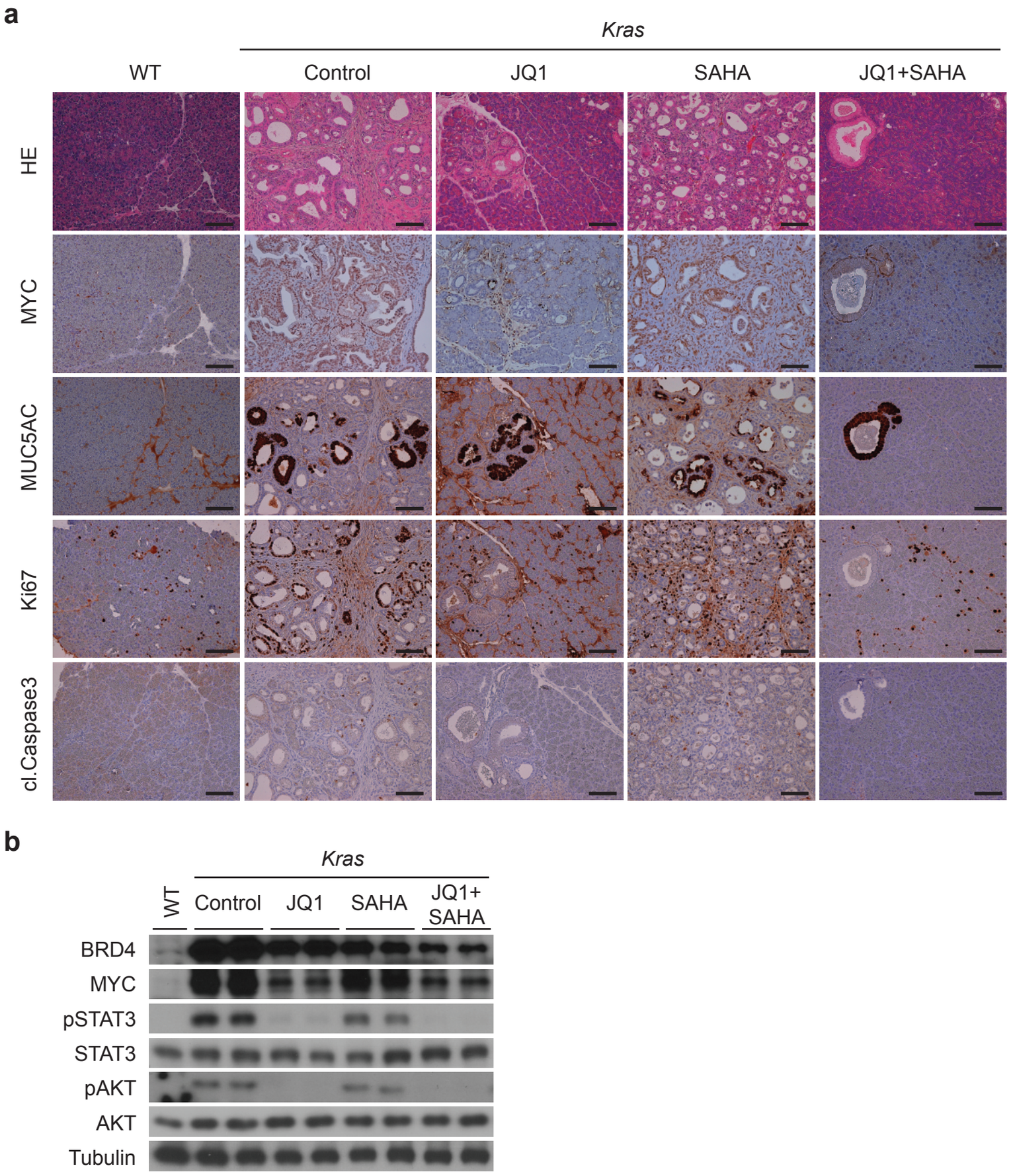

Nature Medicine: doi:10.1038/nm.3952

Supplementary Figure 9. Combined JQ1 and SAHA treatment blocks pancreatitis-induced PanIN formation *in vivo*.

(**a**) Representative HE staining and IHC for MYC, Ki67 (a marker of proliferation), cleaved Caspase 3 (cl.Caspase3, a marker of apoptosis - arrowheads), and MUC5AC (a marker of PanINs) in control and treatment groups as in **Fig.3f–h**. Scale bars, 50 μm.

(**b**) Immunoblot analysis of *Kras* mutant mice control, JQ1 and/or SAHA-treated tumor lysates (each treatment group represents two biological replicates).

Supplementary Figure 10

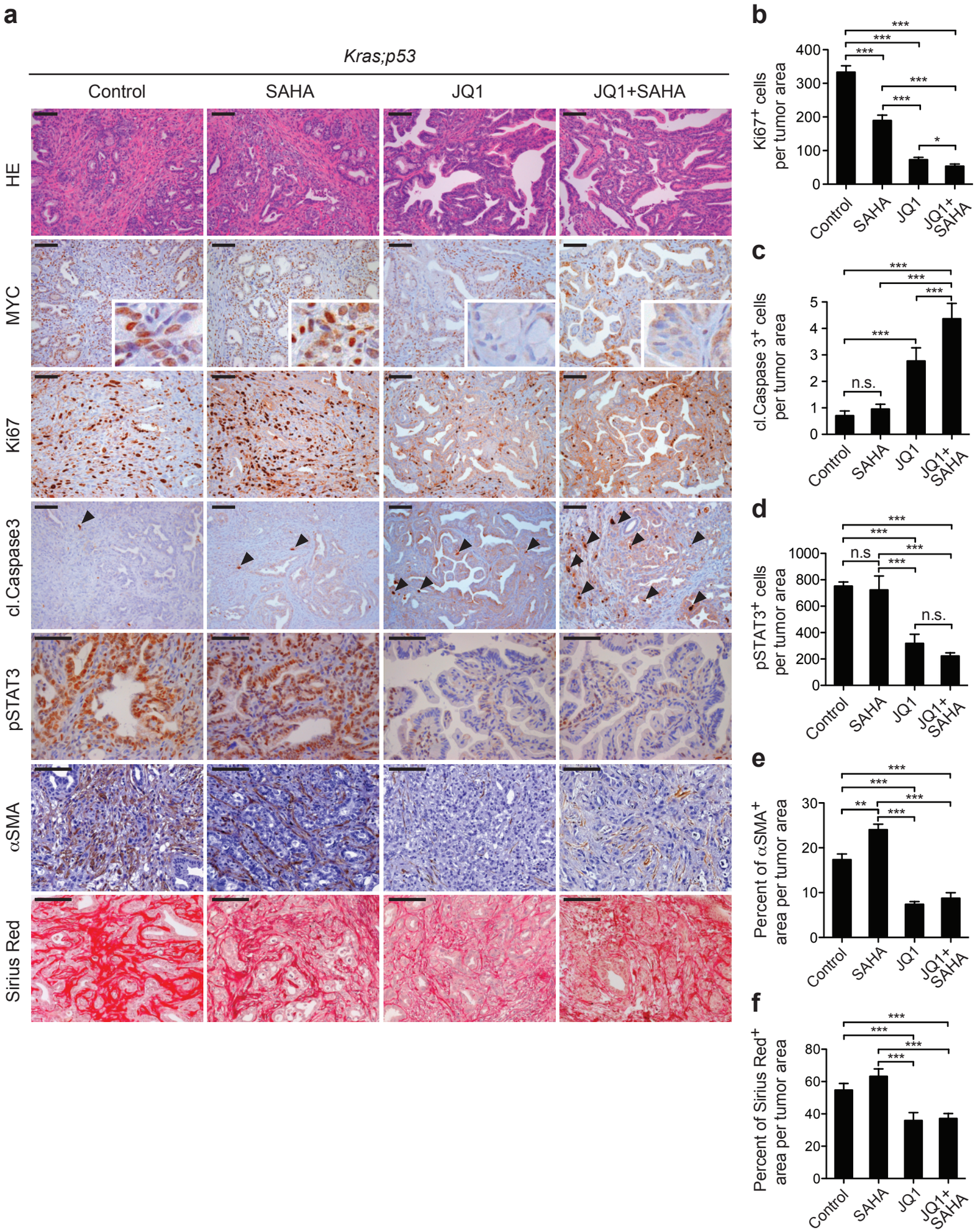

Nature Medicine: doi:10.1038/nm.3952

Supplementary Figure 10. JQ1 and SAHA co-treatment inhibits PDAC growth in *Kras;p53* mutant mice.

(**a**) Representative HE staining and IHC for MYC, Ki67 (a marker of proliferation), cleaved Caspase 3 (cl.Caspase3, a marker of apoptosis - arrowheads), pSTAT3, αSMA (a maker of myofibroblasts/stellate cells) and Sirius Red (a marker of stromal fibrotic deposit) in control and treatment groups. Scale bars, 50 μm.

(**b–d**) Quantification of proliferation (b) (Ki67) and apoptosis (c) (cl.Caspase3), pSTAT3 (d), and tumor-associated stroma (d - αSMA, and e - Sirius Red) (n = 5 for each experimental group). *: $P < 0.05$; **$P < 0.01$; ***: $P < 0.001$; n.s.: not significant (two-tailed unpaired Student's t-test). Data are represented as mean +/– SEM.

Supplementary Figure 11

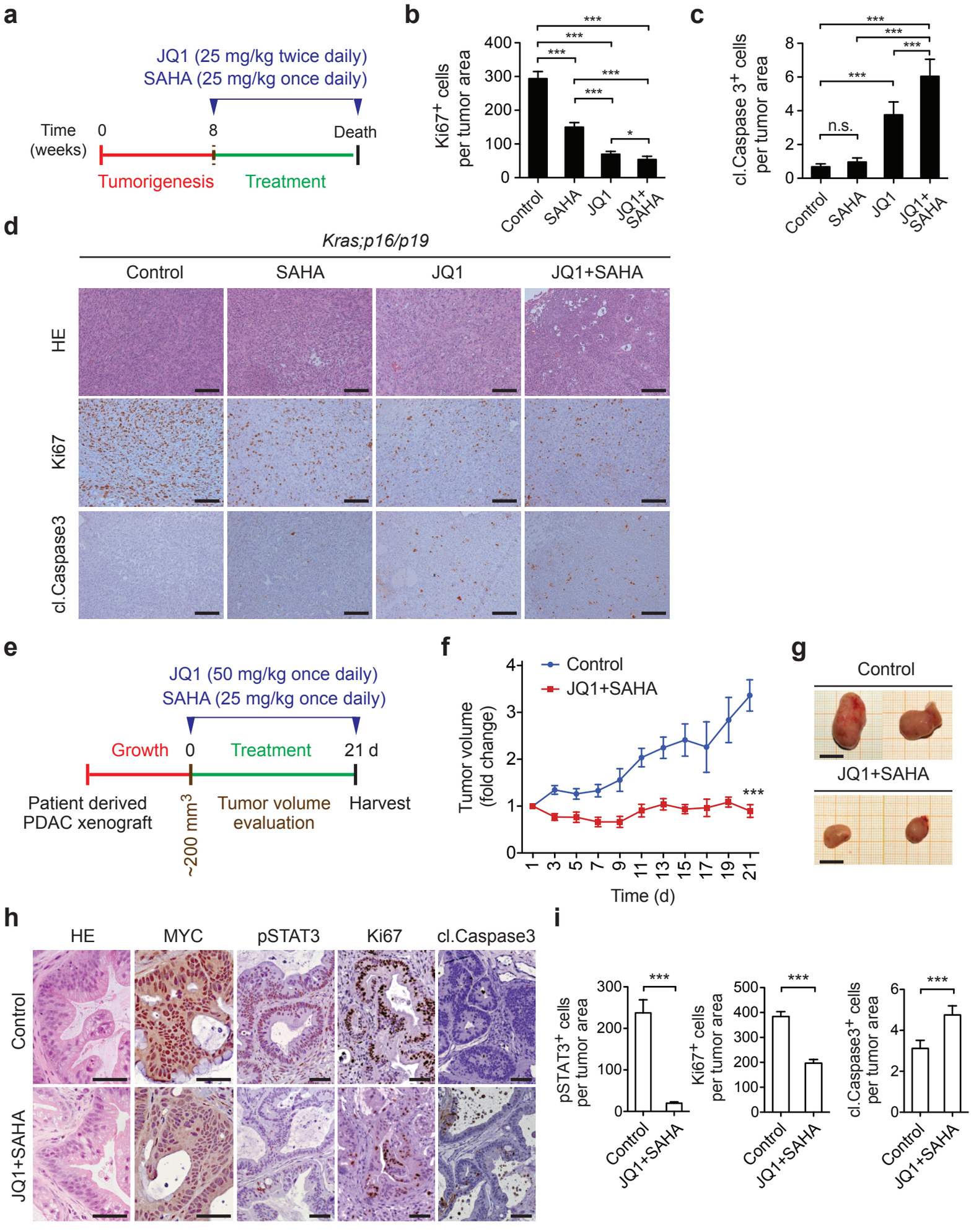

Supplementary Figure 11. JQ1 and SAHA co-treatment inhibits PDAC growth in *Kras;p16/p19* mutant mice and in a patient-derived PDAC xenograft.

(**a**) Treatment schedule for administration of JQ1 and SAHA. Mice undergoing monotherapy also received placebo (vehicle) all *via* intraperitoneal injection.

(**b**) Representative HE staining and IHC for MYC, Ki67 (a marker of proliferation) and cleaved Caspase 3 (cl.Caspase3, a marker of apoptosis - arrowheads) in control and treatment groups. Scale bars, 50 µm.

(**c–d**) Quantification of proliferation (c) (Ki67) and apoptosis (d) (cl.Caspase3), (n = 5 for each experimental group). ***P* < 0.01; ***: *P* < 0.001; n.s.: not significant (two-tailed unpaired Student's t-test). Data are represented as mean +/– SEM.

(**e**) Treatment schedule for administration of JQ1 and SAHA.

(**f**) Tumor volume quantification of the PDAC xenografts in mice (n = 5 mice for each treatment group). ***: *P* < 0.001 (two-tailed unpaired Student's t-test). Data are represented as mean +/– SEM.

(**g**) Representative macroscopic picture of xenografts from control and combined JQ1 and SAHA treatment groups at the end of the experiment. Scale bar, 1 cm.

(**h**) Representative HE staining and IHC for MYC, pSTAT3, Ki67 and cl. Caspase 3 in control and treatment groups. Scale bars, 50 µm.

(**i**) Quantification of pSTAT3, Ki67 and cl. Caspase 3-positive cells per tumor optic field, (n = 5 for each experimental group). ***: *P* < 0.001; n.s.: not significant (two-tailed unpaired Student's t-test). Data are represented as mean +/– SEM.

Supplementary Figure 12

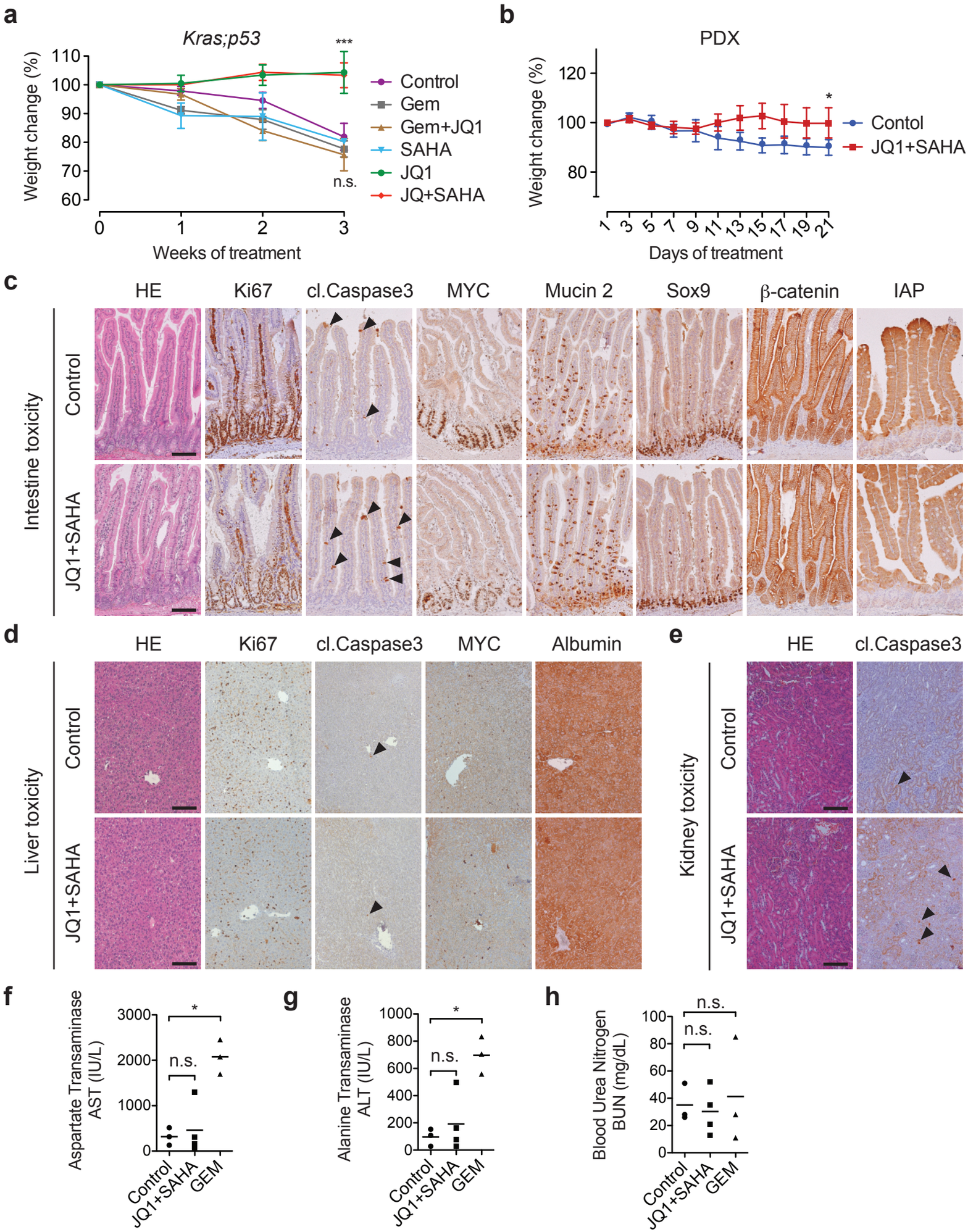

Supplementary Figure 12. JQ1 and SAHA co-treatment has no overt toxicity in mice.
(**a**) Animal weight changes in the course of endogenous PDAC model treatment (n = 4, for each experimental condition). Note that control animals lose weight as a consequence of increased tumor burden (cachectic state) ***: $P < 0.001$; n.s.: not significant (two-tailed unpaired Student's t-test). Data are represented as mean +/– SEM.
(**b**) Animal weight changes in the course of PDX treatment (n = 5, for each experimental condition) *: $P < 0.05$; (two-tailed unpaired Student's t-test). Data are represented as mean +/– SEM.
(**c–e**) Analysis of intestine, liver and kidney toxicity upon JQ1+SAHA treatment. IAP, Intestine Alkaline Phosphatase; arrowheads, positive cl.Caspase3 cells.
(**f–h**) Analysis of serum markers of toxicity in the different treatment groups. GEM, gemcitabine.
*: $P < 0.05$; ns: not significant.

Supplementary Figure 13

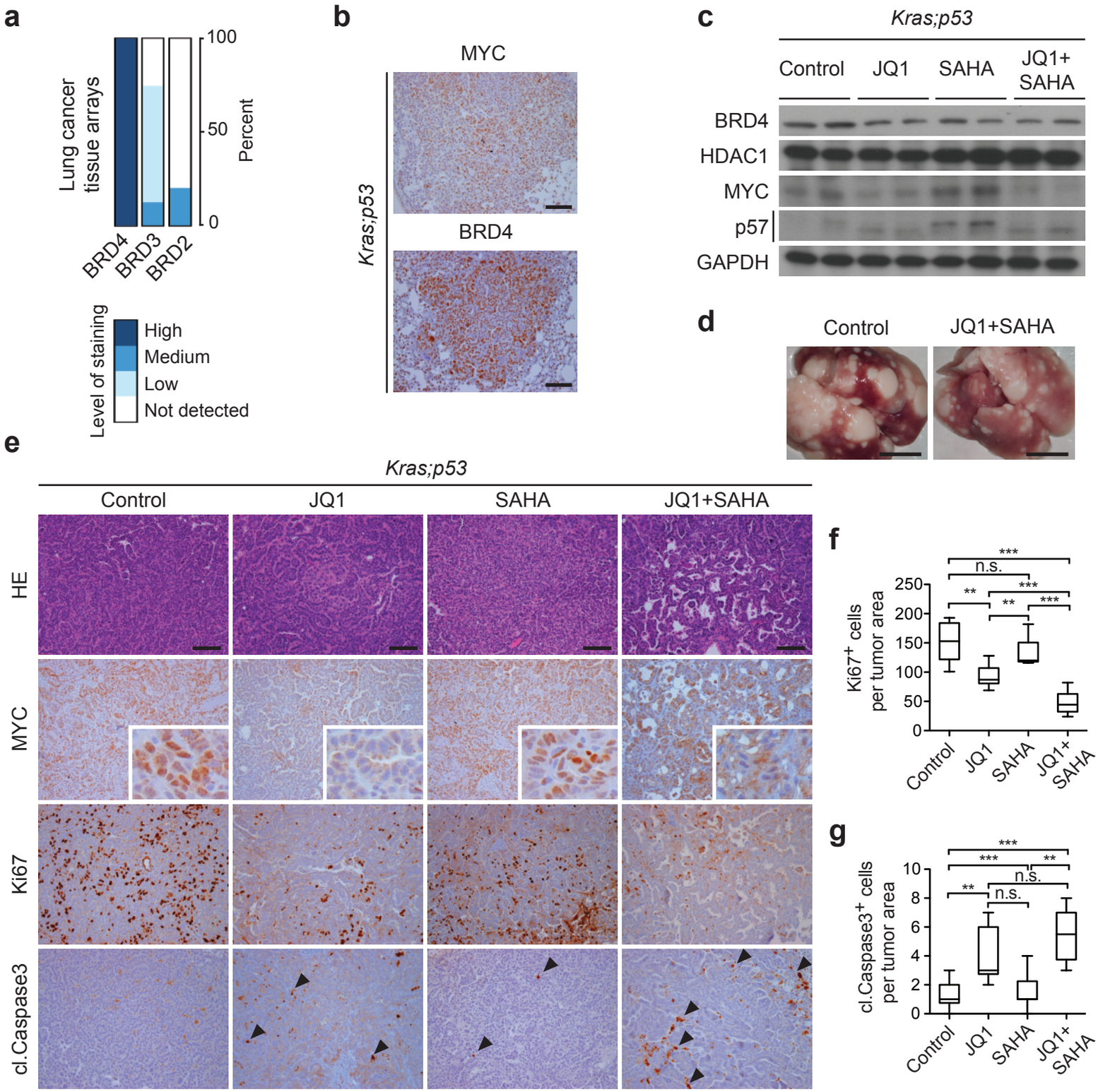

Supplementary Figure 13. JQ1 and SAHA co-treatment inhibits LAC growth in *Kras;p53* mutant mice.

(**a**) BET proteins expression in human lung cancer tissue array (proteinatlas.org).

(**b**) Immunohistochemical analysis of MYC and BRD4 expression in mouse LAC. Scale bars, 50 μm.

(**c**) Immunoblot analysis of lung tumor lysates dissected from *Kras;p53* mutant mice in response to the indicated treatments (two independent biological replicates for each condition).

(**d**) Representative macroscopic picture of lungs of control and treated animals (scale bars, 1 cm)

(**e**) Representative HE staining and IHC for MYC, Ki67 (a marker of proliferation) and cleaved Caspase 3 (cl.Caspase3, a marker of apoptosis - arrowheads) in control and treatment groups. Scale bars, 50 μm.

(**f–g**) Quantification of proliferation (Ki67) and apoptosis (cl.Caspase3), (n = 5 for each experimental group). ***P* < 0.01; ***: *P* < 0.001; n.s.: not significant (two-tailed unpaired Student's t-test). Data are represented as mean +/– SEM.

Supplementary Figure 14

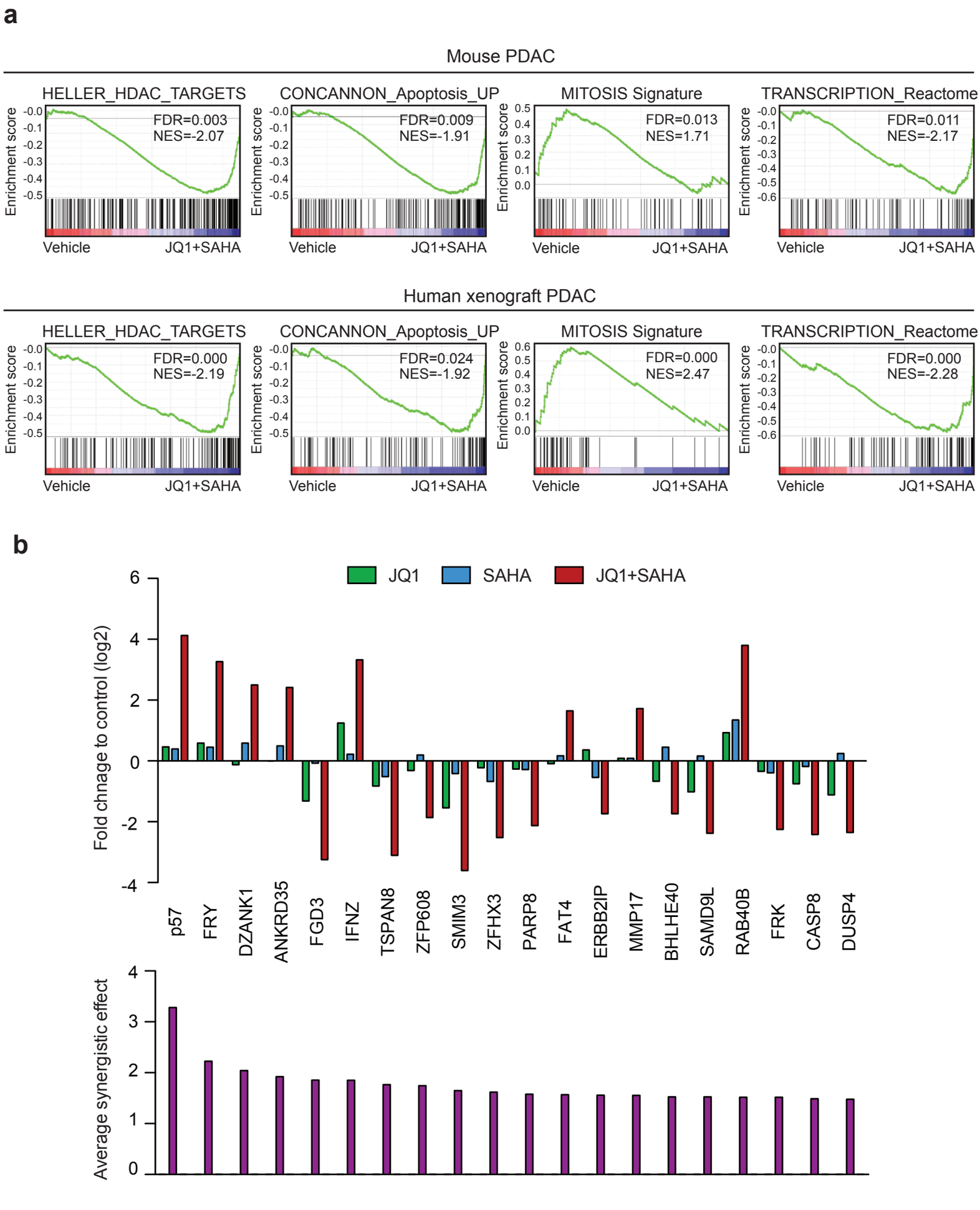

Supplementary Figure 14. JQ1 and SAHA co-treatment synergistically induces multiple changes in the transcriptional profiles of PDAC cells.

(**a**) GSEA on datasets obtained from primary mouse PDAC cells or human xenograft samples treated with vehicle (control, n = 3), and JQ1+SAHA (n = 4).

(**b**) Expression microarray study reveals the top 20 synergistically regulated genes in response to JQ1 and SAHA co-treatment in murine primary PDAC cells. *Cdkn1c* (coding p57/Kip2) was identified as the most synergistically over-expressed gene. Synergy was determined as the excess over the additive expectation. In this case, expression was increased by 0.458 and 0.392 fold in the JQ1 and SAHA treatment groups respectively, leading to an additive expectation of 0.459 + 0.392 = 0.851 (+/–0.173). In the combination treatment, expression increased by 4.129 (+/–0.301), leading to an excess over additivity of 4.129 - 0.851 = 3.278 fold. This increase in expression is validated at the protein level (**Fig. 4a–b**).

Supplementary Figure 15

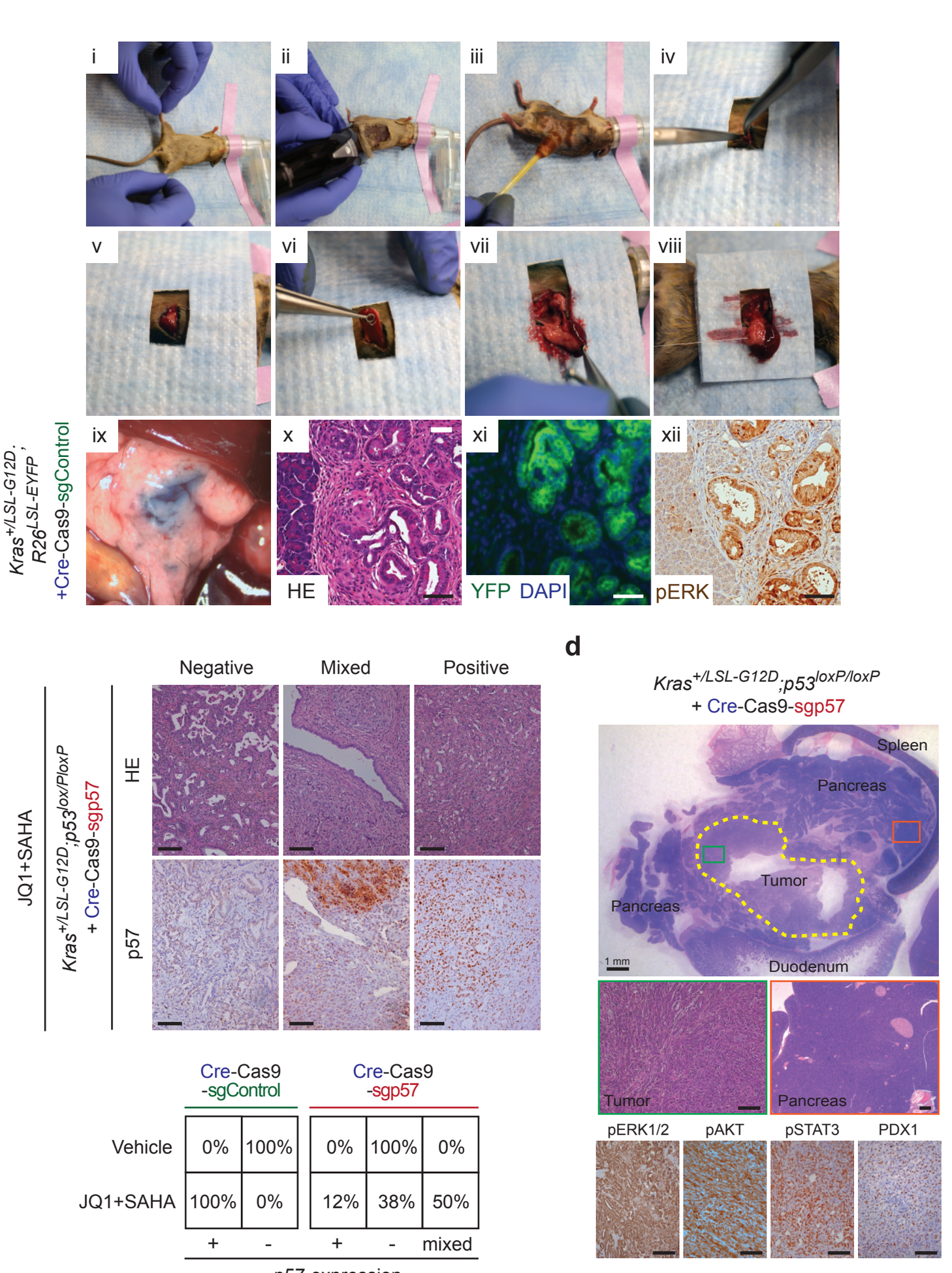

Supplementary Figure 15. A novel CRISPR/Cas9-based mouse model for the rapid investigation of genes involved in PDAC development *in vivo*.

(**a**) Representative images to explain the procedures in mice. Mice are anesthetized (i), the splenic side of abdomen is shaved (ii), disinfected (iii) and a small incision is performed (iv) to expose the pancreas (v), the spleen is pulled (vi) to gain further exposure of the pancreas (vii). The virus is injected into the pancreas parenchyma (viii), a blue dye marks the injection site (ix). The pancreas is then replaced into the abdomen and the wound is sutured. Mice develop localized tumor (x). Recombination is confirmed by activation of EYFP in *Kras;R26*$^{LSL\text{-}EYFP}$ reporter mice (xi) and activation of Ras can be shown by immunostaining for pERK1/2 (xii). All scale bars, 50 μm.

(**b**) Representative HE and p57 IHC staining of serial sections from mouse pancreatic tumors developing after pSECC-sgp57 infection. All scale bars, 50 μm

(**c**) Distribution of p57 IHC staining status in all pSECC-sgCdkn1c (n = 4, vehicle; n = 4, JQ1+SAHA) and pSECC-sgp57 (n = 4, vehicle; n = 8, JQ1+SAHA) infected animals represented as a percent of p57 IHC staining: negative (<30% of the tumor), mixed (30~70% of tumor area) and positive tumors (70~100% of the tumor area).

(**d**) Representative HE image of whole pancreas tissue with tumor area marked with yellow dotted line. Insert (green) shows tumor histology or wild-type area (red) of the injected pancreata. All scale bars, 50 μm, unless marked differently.

Nature Medicine: doi:10.1038/nm.3952